Rate of Access to the Binding Sites in Organically Modified Silicates. 3. Effect of Structure and Density of Functional Groups in Mesoporous Solids Obtained by the Co-Condensation Route

Alain Walcarius* and Cyril Delacôte

Laboratoire de Chimie Physique et Microbiologie pour l'Environnement, Unité Mixte de Recherche UMR 7564, CNRS Université H. Poincaré Nancy I, 405, rue de Vandoeuvre, F-54600 Villers-les-Nancy, France

Received June 4, 2003. Revised Manuscript Received August 21, 2003

Mercaptopropyl-functionalized silica spheres have been prepared by self-assembly co-condensation of mercaptopropyltrimethoxysilane (MPTMS) and tetraethoxysilane (TEOS) precursors in the presence of a cationic surfactant as templating agent and ammonia as catalyst. Several materials have been obtained by varying the MPTMS content from 5 to 100% in the synthesis medium, giving rise to a wide range of porous solids featuring different functionalization levels (denoted MPS-*n*%, with *n* ranging from 5 to 100) and distinct structural order/disorder over different length scales. They were characterized by N_2 sorption isotherms, XRD, scanning and transmission electron microscopy, and particle size analysis. Their reactivity in aqueous media was studied with respect to their binding properties toward Hg^{II} species by complexation with thiol groups. Total accessibility (expressed on the basis of a 1:1 S/Hg stoechiometry) was demonstrated and quantified for well-ordered materials containing up to 30% MPTMS. Less open structures characterized by a high degree of functionalization were subject to less-than-complete sorption capacities, while, however, reaching maximum loading values as high as 750 mg g^{-1}. The speed of the uptake process was studied from batch experiments by using a fast electrochemical technique to monitor the consumption of the reactant, as a function of time, as a consequence of Hg^{II} sorption by the MPS materials. The associated apparent diffusion coefficients were calculated according to a spherical diffusion model, by appropriate fitting of the kinetic curves. They were strongly affected by both the structure and density of functional groups in the MPS sorbents. Whereas the long hexagonally packed one-dimensional channels of MPS-5% and MPS-10% may induce some diffusional restrictions for Hg^{II} to reach the binding sites located deep in the mesopores, transport issues within MPS-15% to MPS-30% sorbents is facilitated by a shorter range structural order in the form of three-dimensional wormhole framework structures. Increasing further the content of organic groups in the materials led to poorly ordered (MPS-40% and MPS-50%) and even amorphous (MPS-70% and MPS-100%) solids, resulting in considerable lowering of mass transfer rates, to which the concomitant increase of hydrophobicity may also contribute to a significant extent. The differences in sorption rates exhibited by MPS materials appear therefore to result from differences in their relative long-range versus short-range structural order/disorder and their intrinsic hydrophobicity, which are induced by their functionalization levels.

1. Introduction

Organic−inorganic hybrid materials that combine in a single solid the structural properties of the rigid inorganic lattice with the intrinsic chemical reactivity of the organic components have generated enormous developments in several scientific disciplines during the past decade, as illustrated in many well-documented reviews.[1−3] Of special interest are those hybrids ascribed to class II,[2a] where the inorganic and organic counterparts are linked via strong-type interactions (covalent or iono-covalent bonds), because they allow durable immobilization of the reactive centers within the material, preventing therefore any leaching event in the surrounding medium. They can be prepared either by post-grafting of as-synthesized materials via reaction with a selected organosilane, or in one step, by co-

* To whom correspondence should be addressed. Fax: (+33) 3 83 27 54 44. E-mail: walcariu@lcpe.cnrs-nancy.fr.

(1) Special issue of *Chem. Mater.* **2001**, *13* (10), 3059−3809.

(2) (a) Sanchez, C.; Ribot, F. *New J. Chem.* **1994**, *18*, 1007. (b) Loy, D. A.; Shea, K. J. *Chem. Rev.* **1995**, *95*, 1431. (c) Schubert, U.; Huesing, N.; Lorenz, A. *Chem. Mater.* **1995**, *7*, 2010. (d) Judeinstein, P.; Sanchez, C. *J. Mater. Chem.* **1996**, *6*, 511. (e) Wen, J.; Wilkes, G. L. *Chem. Mater.* **1996**, *8*, 1667. (f) Corriu, R. J. P.; Leclercq, D. *Angew. Chem., Int. Ed. Engl.* **1996**, *35*, 1421. (g) Chujo, Y. *Curr. Opin. Solid State Mater. Sci.* **1996**, *1*, 806. (h) Rehahn, M. *Acta Polymer.* **1998**, *49*, 201. (i) Sharp, K. G. *Adv. Mater.* **1998**, *10*, 1243. (j) Mackenzie, J. D.; Bescher, E. P. *J. Sol-Gel Sci. Technol.* **1998**, *13*, 371. (k) Gangopadhyay, R.; De, A. *Chem. Mater.* **2000**, *12*, 608. (l) Gomez-Romero, P. *Adv. Mater.* **2001**, *13*, 163.

10.1021/cm031089l CCC: $25.00
Published on Web 09/27/2003

condensation of a tetraalkoxysilane and one (or more) organoalkoxysilane(s). This area has benefitted from the discovery of ordered mesoporous silicas,[4] which has greatly expanded the possibilities for the design of open-pore structures.[3] Organic−inorganic silica-based hybrids are offering opportunities for applications in many fields, such as catalysis,[5] separation sciences,[6] sensors,[7] optics and photonics,[8] electrochemistry,[9] and biology (e.g., bioencapsulation and biosensors),[10] as well as adsorption and pollutant removal for which better performance was achieved with ordered solids displaying regular arrays of uniform-sized channels in comparison to the corresponding amorphous materials.[11]

Two critical parameters governing the performance of organic−inorganic hybrid materials are the accessibility to the active centers and the speed at which reactants can reach these sites within the porous structure (in addition to the particular chemical reactivity that can be tuned by appropriate choice of the organic groups, of course). It has been clearly established that the resort to periodic mesoporous organosilicas, obtained either by post-grafting synthesis[12] or by the co-condensation route,[13] led to better accessibility to the internal organic groups in comparison to that of related amorphous solids.[11] This was mainly demonstrated for the uptake of mercury(II) species by thiol-functionalized mesoporous silica samples, as reported by the groups of Liu, Mercier, and Pinnavaia:[11a−d,e−j,l,m,s,t] access to all the binding sites (100% of SH groups complexed with Hg^{II}) can be achieved in micelle-templated mesostructures with pore diameters larger than 2.0 nm, leading to high capacity adsorbents. The advantage of uniform pore structure was also pointed out in heterogeneous catalysis.[5,14] On the other hand, the speed at which solution-phase species are allowed to move to the active centers located inside the mesoporous structure was only sparingly considered in the literature,[11g,t,15] despite its critical role in applications where mass transport is the rate-determining step, such as electrochemical analysis at chemically modified electrodes[9c−f,16] or pollutant removal from diluted solutions.[11] Kinetics associated with the binding of HgI_4^{2-} species on a mesoporous silica grafted with thiol groups (5-nm pore size) were first qualitatively examined by Mattigod et al.[11g] who have reported rather fast diffusion processes inside the material (80−95% uptake within the first 5 min of reaction). Our group has

(3) (a) Mann, S.; Burkett, S. L.; Davis, S. A.; Fowler, C. E.; Mendelson, N. H.; Sims, S. D.; Walsh, D.; Whilton, N. T. *Chem. Mater.* **1997**, *9*, 2300. (b) Moller, K.; Bein, T. *Chem. Mater.* **1998**, *10*, 2950. (c) Maschmeyer, T. *Curr. Opin. Solid State Mater. Sci.* **1998**, *3*, 71. (d) Sanchez, C.; Lebeau, B.; Ribot, F.; In, M. *J. Sol-Gel Sci. Technol.* **2000**, *19*, 31. (e) Stein, A.; Melde, B. J.; Schroden, R. C. *Adv. Mater.* **2000**, *12*, 1403. (f) Clearfield, A. *Chem. Mater.* **2001**, *13*, 2801. (g) Sayari, A.; Hamoudi, S. *Chem. Mater.* **2001**, *13*, 3151.

(4) (a) Kresge, C. T.; Leonowicz, M. E.; Roth, W. J.; Vartuli, J. C.; Beck, J. S. *Nature* **1992**, *359*, 710. (b) Beck, J. S.; Vartuli, J. C.; Roth, W. J.; Leonowicz, M. E.; Kresge, C. T.; Schmitt, K. D.; Chu, C. T.-W.; Olson, D. H.; Sheppard, E. W.; McCullen, S. B.; Higgins, J. B.; Schlenker, J. L. *J. Am. Chem. Soc.* **1992**, *114*, 10834.

(5) (a) Clark, J. H.; Macquarrie, D. J. *Chem. Commun.* **1998**, 853. (b) Moreau, J. J. E.; Wong Chi Man, M. *Coord. Chem. Rev.* **1998**, *178−180*, 1073. (c) Corma, A. *Top. Catal.* **1998**, *4*, 249. (d) Fajula, F.; Brunel, D. *Microporous Mesoporous Mater.* **2001**, *48*, 119. (e) Brunel, D. *Sp. Pub. Royal Soc. Chem.* **2001**, *266*, 38. (f) Brunel, D.; Blanc, A. C.; Galarneau, A.; Fajula, F. *Catal. Today* **2002**, *73*, 139. (g) Wight, A. P.; Davis, M. E. *Chem. Rev.* **2002**, *102*, 3589. (h) Valkenberg, M. H.; Holderich, W. F. *Catal. Rev. Sci. Eng.* **2002**, *44*, 321.

(6) (a) Linden, M.; Schacht, S.; Schüth, F.; Steel, A.; Unger, K. K. *J. Porous Mater.* **1998**, *5*, 177. (b) Inagaki, S.; Ogata, S.; Goto, Y.; Fukushima, Y. *Stud. Surf. Sci. Catal.* **1998**, *117*, 65. (c) Mauritz, K. A. *Mater. Sci. Eng.* **1998**, *C6*, 121. (d) Liu, J.; Fryxell, G. E.; Mattigod, S.; Zemanian, T. S.; Shin, Y.; Wang, L.-Q. *Stud. Surf. Sci. Catal.* **2000**, *129*, 729. (e) Guizard, C.; Bac, A.; Barboiu, M.; Hovnanian, N. *Mol. Cryst. Liq. Cryst. Sci. Technol., A* **2000**, *354*, 91. (f) Kisler, J. M.; Dahler, A.; Stevens, G. W.; O'Connor, A. J. *Microporous Mesoporous Mater.* **2001**, *44−45*, 769. (g) Ruiz-Hitzky, E.; Casal, B.; Aranda, P.; Galvan, J. C. *Rev. Inorg. Chem.* **2001**, *21*, 125. (h) Malik A. *Electrophoresis* **2002**, *23*, 3973.

(7) (a) Lev, O.; Tsionsky, M.; Rabinovich, L.; Glezer, V.; Sampath, S.; Pankratov, I.; Gun, J. *Anal. Chem.* **1995**, *67*, 22A. (b) Livage, J. *NATO ASI Ser., Ser. E* **1995**, *297*, 3. (c) Bescher, E.; Mackenzie, J. D. *Mater. Sci. Eng.* **1998**, *C6*, 145. (d) Collinson, M. M. *Mikrochim. Acta* **1998**, *129*, 149.

(8) (a) Seddon, A. B. *Crit. Rev. Optical Sci. Technol.* **1997**, *CR68*, 143. (b) Gvishi, R.; Narang, U.; Ruland, G.; Kumar, D. N.; Prasad, P. N. *Appl. Organomet. Chem.* **1997**, *11*, 107. (c) Lebeau, B.; Sanchez, C. *Curr. Opin. Solid State Mater. Sci.* **1999**, *4*, 11. (d) Sanchez, C.; Ribot, F.; Lebeau, B. *J. Mater. Chem.* **1999**, *9*, 35. (e) Sanchez, C.; Lebeau, B.; Ribot, F.; In, M. *J. Sol-Gel Sc. Technol.* **2000**, *19*, 31. (f) Sanchez, C.; Lebeau, B. *MRS Bull.* **2001**, *26*, 377.

(9) (a) Lev, O.; Wu, Z.; Bharathi, S.; Glezer, V.; Modestov, A.; Gun, J.; Rabinovich, L.; Sampath, S. *Chem. Mater.* **1997**, *9*, 2354. (b) Alber, K. S.; Cox, J. A. *Mikrochim. Acta* **1997**, *127*, 131. (c) Walcarius, A. *Electroanalysis* **1998**, *10*, 1217. (d) Walcarius, A. *Electroanalysis* **2001**, *13*, 701. (e) Walcarius, A. *Chem. Mater.* **2001**, *13*, 3351. (f) Rabinovich, L.; Lev, O. *Electroanalysis* **2001**, *13*, 265.

(10) (a) Wang, J. *Anal. Chim. Acta* **1999**, *399*, 21. (b) Pandey, P. C. *J. Indian Inst. Sci.* **1999**, *79*, 415. (c) Gill, I. *Chem. Mater.* **2001**, *13*, 3404. (d) Jin, W.; Brennan, J. D. *Anal. Chim. Acta* **2002**, *461*, 1.

(11) See, e.g., (a) Feng, X.; Fryxell, G. E.; Wang, L.-Q.; Kim, A. Y.; Liu, J.; Kemmer, K. M. *Science* **1997**, *276*, 923. (b) Mercier, L.; Pinnavaia, T. J. *Adv. Mater.* **1997**, *9*, 500. (c) Mercier, L.; Pinnavaia, T. J. *Environ. Sci. Technol.* **1998**, *32*, 2749. (d) Liu, J.; Feng, X.; Fryxell, G. E.; Wang, L.-Q.; Kim, A. Y.; Gong, M. *Adv. Mater.* **1998**, *10*, 161. (e) Zhao, X. S.; Lu, G. Q. *J. Phys. Chem. B* **1998**, *102*, 1556. (f) Chen, X.; Feng, X.; Liu, J.; Fryxell, G. E.; Gong, M. *Sep. Sci. Technol.* **1999**, *34*, 1121. (g) Mattigod, S. V.; Feng, X.; Fryxell, G. E.; Liu, J.; Gong, M. *Sep. Sci. Technol.* **1999**, *34*, 2329. (h) Fryxell, G. E.; Liu, J.; Hauser, T. A.; Nie, Z.; Ferris, K. F.; Mattigod, S.; Gong, M.; Hallen, R. T. *Chem. Mater.* **1999**, *11*, 2148. (i) Brown, J.; Mercier, L.; Pinnavaia, T. J. *Chem. Commun.* **1999**, 69. (j) Feng, X.; Rao, L.; Mohs, T. R.; Xu, J.; Xia, Y.; Fryxell, G. E.; Liu, J.; Raymond, K. N. *Ceramic Trans.* **1999**, *93*, 35. (k) Ju, Y. H.; Webb, O. F.; Dai, S.; Lin, J. S.; Barnes, C. E. *Int. Eng. Chem. Res.* **2000**, *39*, 550. (l) Brown, J.; Richer, R.; Mercier, L. *Microporous Mesoporous Mater.* **2000**, *37*, 41. (m) Fryxell, G. E.; Liu, J.; Mattigod, S. V.; Wang, L. Q.; Gong, M.; Hauser, T. A.; Lin, Yuehe; Ferris, K. F.; Feng, X. *Ceramic Trans.* **2000**, *107*, 29. (n) Seneviratne, J.; Cox, J. A. *Talanta* **2000**, *52*, 801. (o) Liu, A. M.; Hidajat, K.; Kawi, S.; Zhao, D. Y. *Chem. Commun.* **2000**, 1145. (p) Ju, Y. H.; Webb, O. F.; Dai, S.; Lin, J. S.; Barnes, C. E. *Int. Eng. Chem. Res.* **2000**, *39*, 550. (q) Lin, Y.; Fryxell, G. E.; Wu, H.; Engelhard, M. *Environ. Sci. Technol.* **2001**, *35*, 3962. (r) Lee, B.; Kim, Y.; Lee, H.; Yi, J. *Microporous Mesoporous Mater.* **2001**, *50*, 77. (s) Huq, R.; Mercier, L.; Kooyman, P. J. *Chem. Mater.* **2001**, *13*, 4512. (t) Bibby, A.; Mercier, L. *Chem. Mater.* **2002**, *14*, 1591. (u) Etienne, M.; Sayen, S.; Lebeau, B.; Walcarius A. *Stud. Surf. Sci. Catal.* **2002**, *141*, 615.

(12) (a) Liu, J.; Feng, X. D.; Fryxell, G. E.; Wang, L. Q.; Kim, A. Y.; Gong, M. L. *Adv. Mater.* **1998**, *10*, 161. (b) Impens, N. R. E. N.; Van der Voort, P.; Vansant, E. F. *Microporous Mesoporous Mater.* **1999**, *28*, 217. (c) Brunel, D. *Microporous Mesoporous Mater.* **1999**, *27*, 329. (d) Clark, J. H.; Macquarrie, D. J.; Wilson, K. *Stud. Surf. Sci. Catal.* **2000**, *129*, 251.

(13) (a) Burkett, S. L.; Sims, S. D.; Mann, S. *Chem. Commun.* **1996**, 1367. (b) Macquarrie, D. J. *Chem. Commun.* **1996**, 1961. (c) Fowler, C. E.; Mann, S.; Lebeau, B. *Chem. Commun.* **1998**, 1825. (d) Asefa, T.; Yoshina-Ishii, C.; MacLachlan, M. J.; Ozin, G. A. *J. Mater. Chem.* **2000**, *10*, 1751. (e) Burleigh, M. C.; Markowitz, M. A.; Spector, M. S.; Gaber, B. P. *J. Phys. Chem. B* **2001**, *105*, 9935.

(14) (a) Maschmeyer, T.; Rey, F.; Sankar, G.; Thomas, J. M. *Nature* **1995**, *378*, 159. (b) Macquarrie, D. J.; Jackson, D. B. *Chem. Commun.* **1997**, 1781. (c) Bossaert, W.; De Vos, D. E.; Van Rhijn, W. M.; Bullen, J.; Grobet, P. J.; Jacobs, P. A. *J. Catal.* **1999**, *182*, 156. (d) Pinnavaia, T. J.; Pauly, T. R.; Kim, S. S. *Sp. Pub. Royal Soc. Chem.* **2001**, *266*, 19.

(15) (a) Walcarius, A.; Etienne, M.; Bessière, J. *Chem. Mater.* **2002**, *14*, 2757. (b) Walcarius, A.; Etienne, M.; Lebeau, B. *Chem. Mater.* **2003**, *15*, 2161.

(16) (a) Walcarius, A.; Despas, C.; Trens, P.; Hudson, M. J.; Bessière, J. *J. Electroanal. Chem.* **1998**, *453*, 249. (b) Walcarius, A.; Lüthi, N., Blin, J.-L.; Su, B.-L.; Lamberts, L. *Electrochim. Acta* **1999**, *44*, 4601. (c) Villemure, G.; Pinnavaia, T. J. *Chem. Mater.* **1999**, *11*, 789. (d) Walcarius, A.; Bessière, J. *Chem. Mater.* **1999**, *11*, 3009. (e) Etienne, M.; Bessière, J.; Walcarius, A. *Sensors Actuators B* **2001**, *76*, 531. (f) Sayen, S.; Etienne, M.; Bessière, J.; Walcarius A. *Electroanalysis* **2002**, *14*, 1521. (g) Walcarius A.; Etienne, M.; Sayen, S.; Lebeau, B. *Electroanalysis* **2003**, *15*, 414.

provided a more quantitative approach, which was applied to the study of diffusion processes of several reactants (H^+, Cu^{II}, Hg^{II}) in various silica samples grafted with either aminopropyl or mercaptopropyl groups, ranging from amorphous silica gels with different porosity[15a] to ordered mesoporous silicas of different structure and pore size.[15b] It was demonstrated that the reaction rates were usually higher in well-organized internal porous structures than in amorphous particles (of similar pore size), because of lower resistance to diffusion in the former case. After appropriate fitting of the experimental kinetic curves, it was possible to evaluate the apparent diffusion coefficients in the materials. They were found to be affected by several parameters (such as pore size of the adsorbent, density of organic groups in the hybrid, structure of the material, size, and charge of the reactant) and decreased as the extent of reaction increased, especially at high loadings.[15] Finally, by studying Hg^{II} adsorption in thiol-functionalized mesoporous silica spheres of big size (10−12 μm) and applying another kinetic model, Bibby and Mercier[11t] have observed a different trend in which the diffusion coefficient values were increasing as a function of time, suggesting an apparent acceleration of the uptake process upon filling the adsorbent.

To go one step further in comparison to our previous works dealing with diffusion kinetics in grafted silicas (amorphous or ordered),[15] we provide here a detailed study of accessibility and mass transport rates in organic−inorganic hybrids prepared by the co-condensation route. Mesoporous materials prepared by this direct assembly pathway are characterized by a regular distribution of organic groups, in a more uniform way than that obtained by the postsynthesis grafting.[17] For the purposes of the present investigation, the selected process was the uptake of Hg^{II} species from aqueous solutions by complexation to thiol groups anchored into silica matrixes prepared by the sol−gel method in the presence of a surfactant template. Materials synthesis was performed from mixtures of 3-mercaptopropyltrimethoxysilane (MPTMS) and tetraethoxysilane (TEOS) in the presence of a cationic surfactant, in conditions leading to the production of organically modified mesoporous silica spheres, according to our recently published procedure.[18] To elucidate the influence of various factors that are expected to affect the mercury uptake efficiency, several adsorbent samples have been prepared from starting sols containing MPTMS and TEOS in various ratios (ranging from 0% to 100% MPTMS), which is expected to give materials displaying very different structures and properties (ordered or amorphous, long-range or short-range order, wide range of organic group contents, variable hydrophobicity, etc.). The choice of this system was otherwise dictated by the fact that mercapto-functionalized mesoporous silicas have received considerable attention as heavy-metal trapping agents.[11a−d,e−j,l−n,s−u] After a thorough examination of the materials structure and properties by various physicochemical techniques, the Hg^{II} adsorption isotherms will be constructed in both lack and excess of reactant with respect to the theoretical maximal capacity of the adsorbents, and kinetic uptake profiles will be determined by using a previously developed electrochemical method[15] enabling a fast and continuous monitoring of the uptake process with time. The apparent diffusion coefficients will be calculated according to a spherical diffusion model, and results will be discussed by taking into account the various structural and chemical characteristics of the adsorbents. Comparison to the corresponding grafted materials also will be provided.

2. Experimental Section

2.1. Chemicals and Reagents. Mercury(II) solutions were obtained from its nitrate salt ($Hg(NO_3)_2$ —***attention, mercury is highly toxic***—, which was purchased from Prolabo. They were prepared daily by diluting a stock solution of 0.10 M (in 0.1 M HNO_3) in high purity water (18 MΩ cm) obtained from a Millipore Milli-Q water purification system. Their concentration was checked using a certified standard solution, at 1.001 ± 0.002 g L^{-1} Hg^{II}, which was purchased from Merck. All other reagents were analytical grade and all solutions were prepared with high purity water.

Analytical-grade chemicals from the following suppliers were used as purchased for all solid sample preparations: tetraethoxysilane (TEOS, >98%, Merck), mercaptopropyltrimethoxysilane (MPTMS, 95%, Lancaster), cetyltrimethylammonium bromide (CTAB, 98%, Fluka), ammonia (28% aqueous, Prolabo), ethanol (95−96%, Merck), and HCl (37%, Prolabo).

2.2. Preparation of Thiol-Functionalized Hybrid Materials. One-pot syntheses of thiol-functionalized silicas were performed according to our previously published procedure, which was designed to get organically modified mesoporous silica spheres with MCM-41 architecture.[18] In this case, however, samples containing higher and variable concentrations of mercaptopropyl groups have been prepared. The typical molar composition of reagents was 1:0.41:11.8:65:175 precursors/CTAB/ammonia/ethanol/water, with precursors made of MPTMS/TEOS ratios varying from 0 to 100%. CTAB (2.4 g) was dissolved in 50 mL of deionized water and 45 mL of ethanol (95−96%) to which 13 mL of 28% aqueous ammonia was added. The precursor mixture was prepared by dissolving appropriate ratios of MPTMS and TEOS in 5 mL of ethanol, which was then added to the surfactant-plus-catalyst solution under vigorous stirring. Condensation occurred within 2 min. The resulting white precipitate was stirred for 2 h at room temperature. The product was then isolated by vacuum filtration on a Büchner funnel and washed alternatively with water and ethanol. The resulting powder was dried under vacuum ($<10^{-2}$ bar) for 24 h. The surfactant was removed from the hybrid material by acid/solvent extraction by suspending the solid particles in 1 M HCl in ethanol (1 g solid in 100 mL solution), which was then allowed to reflux during 18 h. After the solution was filtered and washed with ethanol, the solid was dried according to the aforementioned conditions. The functionalized materials have been named herein as MPS (mercaptopropyl-silica), followed by the MPTMS ratio in the starting sol (MPS-0% or MCM-41, MPS-5%, MPS-10%, MPS-15%, MPS-20%, MPS-25%, MPS30%, MPS-40%, MPS-50%, MPS-70%, and MPS-100%). The amount of organic groups in the final materials was determined from elemental analyses performed at the Service Central d'Analyse of the CNRS at Lyon, France.

For comparison purposes, three other silica samples grafted with mercaptopropyl groups were also used: a small-pore MCM-41 (∼35 Å pore size), a large-pore SBA-15 (∼65 Å pore size), and an amorphous silica gel (SI60 from Geduran, ∼75 Å pore size). They have been obtained as previously described.[15] The resulting grafted solids contain respectively 1.5, 1.0, and 1.5 mmol SH group per gram; they are characterized

(17) (a) Lim, M. H.; Stein, A. *Chem. Mater.* **1999**, *11*, 3285. (b) Mercier, L.; Pinnavaia, T. J. *Chem. Mater.* **2000**, *12*, 188. (c) Corriu, R. J. P.; Lancelle-Beltran, E.; Mehdi, A.; Reyé, C.; Brandès, S.; Guilard, R. *J. Mater. Chem.* **2002**, *12*, 1355.

(18) Etienne, M.; Lebeau, B.; Walcarius, A. *New J. Chem.* **2002**, *26*, 384.

by specific surface areas of 818 $m^2\ g^{-1}$ (MCM-41-SH), 467 $m^2\ g^{-1}$ (SBA-15-SH), and 314 $m^2\ g^{-1}$ (Geduran-SH), and average particle sizes of 8, 6, and 63 μm, respectively.

2.3. Instrumentation. Powder X-ray diffraction data were collected at room temperature using a classical powder diffractometer (X'PERT PRO, Philips), equipped with a Cu anode (quartz monochromator, $K\alpha_1$ radiation, $\lambda = 0.154056$ nm). Nitrogen adsorption−desorption measurements were performed at 77 K with a Coulter instrument (model SA 3100), in the relative pressure range from about 10^{-5} to 0.99. Specific surface areas and pore sizes were calculated by the BET and BJH methods, respectively. All samples were dried at 50 °C for a minimum of 12 h under vacuum before carrying out the nitrogen adsorption experiments. Scanning electron microscopy (SEM) was performed with a Philips XL30 apparatus, and transmission electron microscopy (TEM) pictures were obtained from a Philips CM20 microscope operating at 200 keV. Particle size distribution was measured with using a light scattering analyzer (model LA920, Horiba), based on the Mie scattering theory.

2.4. Procedures. *2.4.1. Batch Experiments: Adsorption Isotherms at Various Mercury(II) Concentrations.* The maximum capacity of materials for mercury(II) species was determined after 24 h reaction in a medium containing the reactant in excess, by solution phase analysis of the remaining reactant concentration. Quantitative analysis of mercury(II) in solution was carried out by anodic stripping differential pulse voltammetry on gold electrode,[19] using a μ-Autolab potentiostat associated with the GPES electrochemical analysis system (Eco Chemie). Measurements were performed in a conventional single-compartment cell assembled with a rotating gold electrode, an Ag/AgCl reference electrode (Metrohm, 6.0733.100), and a Pt wire auxiliary electrode. The electrolyte medium was made of 1.2 10^{-3} M EDTA (ethylenediaminetetraacetate, disodium form, 99%, from Prolabo), 7.2 10^{-3} M NaCl (Prolabo), and 2.8 10^{-4} M $HClO_4$ (Riedel-de Haën). Stripping voltammograms were recorded after 30-s electrolysis at +0.3 V, by scanning potentials in the differential pulse mode up to +0.8 V. Analysis was performed after appropriate dilution (if necessary) to fall into the linear range of the technique (0.1−1 μM). The maximum capacity results obtained from solution-phase Hg^{II} determination were confirmed by solid-phase analysis of Hg^{II} adsorbed on the materials, which was performed by the Service Central d'Analyse of the CNRS at Lyon, France.

The same analytical technique was applied to construct the sorption isotherms for Hg^{II} on MPS materials. Typically, 20 mgof solid was suspended in 20 mL of solutions containing various Hg^{II} concentrations in the 0.05−20 mM range (in 0.1 M HNO_3), to cover wide experimental conditions extending from lack to large excess of reactant with respect to the amounts of thiol groups in the materials. The suspensions were allowed to react under stirring during 24 h, the solids were then filtered off, and the remaining Hg^{II} concentrations in solution were determined by the aforementioned method after appropriate dilution if necessary. The amounts of adsorbed Hg^{II} were calculated by difference from the starting concentrations and expressed by mass of MPS material.

2.4.2. Kinetic Experiments: Adsorption of Mercury(II) as a Function of Time. Because the uptake processes were often very fast, an electrochemical method recently developed by our group[15] was used to continuously monitor the solution-phase Hg^{II} directly in MPS suspensions, which was preferred over intermittent concentration measurements (discontinuous analysis of remaining Hg^{II} in solution after solid filtration, which was used elsewhere[11g,t]). The method is based on the continuous amperometric analysis of Hg^{II} species at a rotating disk electrode in conditions where steady-state currents are directly proportional to their concentration. Briefly, a constant potential of −0.5 V (vs SCE) is applied to a glassy carbon rotating disk electrode (rotation speed 2000 rd min^{-1}) until reaching a steady-state current in a 200-mL solution containing Hg^{II} at a selected starting concentration (in 0.1 M HNO_3). A weighed amount of MPS is then added into the cell, after being previously dispersed in a 5-mL aliquot of water under sonication to ensure a steady-state distribution of particle size, and Hg^{II} consumption is measured by recording the decrease in transient currents at the rotating electrode (two sampling points per second). Particle size distributions are measured afterward. Other calibration details and control experiments have been reported previously.[15a] The experiments have been carried out at room temperature in an undivided three-electrode cell using a model 283 potentiostat/galvanostat from EG&G Princeton Applied Research (PAR), monitored by the M270 electrochemical research software (EG&G PAR). The reference was the silver/silver chloride electrode (Ag/AgCl).

2.4.3. Kinetic Data Treatment. The rate of Hg^{II} uptake by MPS materials is expected to be the physical diffusion of the analytes inside the organically modified porous structures. This rate-determining step is mainly affected by the particle size (and shape) and the apparent diffusion coefficient of the analyte inside the particle. From measurements of both particle size distribution and Hg^{II} sorption data as a function of time, it is possible to estimate the apparent diffusion coefficient of reactive species within the material. This is done by plotting kinetic data in the form of the variation of Q/Q_0 ratios with time, where Q is the amount of reactant that has reached the binding sites within/on the solid particles at time t, and Q_0 is the maximum amount of accessible binding sites for the target analyte species (i.e., the amount of sorbed Hg^{II} after 24 h). These curves were then fitted to a spherical non-steady-state diffusion model[20] by assuming a homogeneous distribution of thiol groups inside the porous material (which is an acceptable hypothesis for hybrids obtained by the co-condensation route[17]), according to eq 1 as established in the form of level-headed sum of each contribution of populations displaying the same particle size a_x, which was applied earlier to both amorphous and ordered silicas grafted with amine or thiol groups.[15]

$$\frac{Q}{Q_0} = \sum_{x=1}^{x=n} f_{a_x}\left[6\left(\frac{Dt}{a_x^2}\right)^{1/2}\left\{\pi^{-1/2} + 2\sum_{n=1}^{\infty}(-1)^n ierfc\,\frac{na_x}{\sqrt{Dt}}\right\} - 3\frac{Dt}{a_x^2}\right] \quad (1)$$

where Q/Q_0 has been defined above, D is the apparent diffusion coefficient (denoted D_{app} hereafter), a is the particle size radius, *ierfc* is the error function, t is time, and f_{ax} is the relative fraction of particles having the same size a_x. This fraction ranges from 0 to 1 and is determined from particle size distribution measurements.

3. Results and Discussion

3.1. Characterization of Materials. The mercaptopropylsilyl-functionalized silica-based materials have been prepared through a direct assembly pathway at room temperature in the presence of a surfactant template (CTAB) in conditions leading to the formation of regular spheres with internal mesostructure (ammonia catalyst in water/ethanol medium).[18] A wide range of functionalized solids was synthesized over the full stoichiometric range of 0−100% MPTMS in the starting mixture relative to the whole precursors content (MPTMS + TEOS). Their main physicochemical characteristics are summarized in Table 1.

In agreement with previous reports describing the preparation of similar materials by other routes (acid

(19) Bonfil, Y.; Brand, M.; Kirowa-Eisner, E. *Anal. Chim. Acta* **2000**, *424*, 65.

(20) Crank, J. *The Mathematics of Diffusion*; Clarendon Press: Oxford, 1975.

Table 1. Physicochemical Characteristics of Mercaptopropyl Silica Samples

	powder XRD	nitrogen adsorption			average particle size[c]		
sample	*d* spacing (Å)	BET surface area ($m^2\ g^{-1}$)	total pore volume ($cm^3\ g^{-1}$)	average pore size[b] (Å)	isolated particle (μm)	aggregates (μm)	amount of mercaptopropyl groups (mmol g^{-1})
MCM-41	35	1264	0.87	27	0.56	5.8 ± 1.4	0.00
MPS-5%	34	1431	0.81	23	0.59	5.5 ± 1.2	0.53
MPS-10%	33	1598	0.76	20	0.62	6.5 ± 1.9	0.89
MPS-15%	31	1269	0.58	< 20	0.61	5.4 ± 1.1	1.55
MPS-20%	29	1073	0.50	< 20	0.58	6.4 ± 1.1	2.26
MPS-25%	29	819	0.41	< 20	0.56	6.7 ± 0.5	2.59
MPS-30%	28	757	0.38	< 20	0.55	9.3 ± 1.4	3.18
MPS-40%	27	474	0.25	< 20	0.52	12.4 ± 1.2	4.03
MPS-50%	25	340	0.18	< 20	0.50	15.9 ± 1.1	4.69
MPS-70%	nm[a]	3.4	0.01	nm[a]	0.51	14.8 ± 0.7	6.1
MPS-100%	nm[a]	2.5	0.01	nm[a]	0.44	22.0 ± 2.0	7.0

[a] Not measurable. [b] Determined from the BJH method. [c] From triplicate measurements. [d] Expressed per gram of functionalized material.

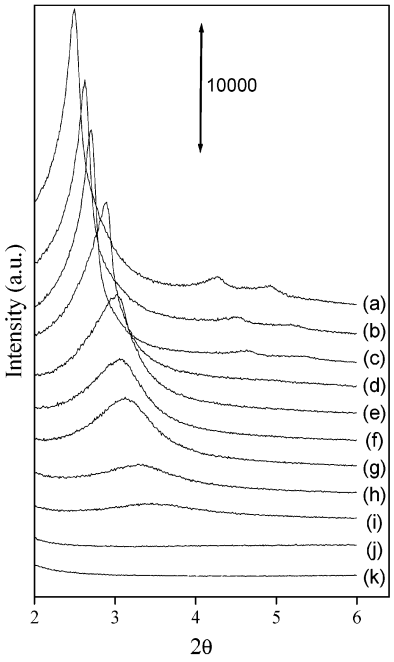

Figure 1. Powder X-ray diffraction patterns for cetyltrimethylammonium-assembled nanoporous silica derivatives, organically modified with mercaptopropyl groups (MPS), which are depicted as a function of the molar percent of MPTMS in the starting sol: (a) MCM-41 (0%), (b) MPS-5%, (c) MPS-10%, (d) MPS-15%, (e) MPS-20%, (f) MPS-25%, (g) MPS-30%, (h) MPS-40%, (i) MPS-50%, (j) MPS-70%, and (k) MPS-100%.

or base catalysis, different structure-directing agents, and variable temperature),[17b,21,22] the framework mesostructures were better expressed at low organic group contents. Figure 1 depicts the powder XRD patterns for most of the samples synthesized in this work. They can be distinguished into several categories. The pure silica solid and those containing low thiol contents (MPS-5% and MPS-10%) display a typical hexagonal MCM-41 structure, with XRD patterns featuring one main correlation reflection at 2θ angles between 2° and 3° and two weaker reflections at higher 2θ angles, corresponding respectively to diffraction plans that could be indexed as *100*, *110*, and *200*. The hexagonal structure was also evidenced by high resolution TEM, as illustrated in Figure 2 for the pure silica MCM-41 (part a) and the MPS-5% sample (part b). The regular mesostructure was maintained after template removal. At such low loadings of mercaptopropyl groups, the framework pore sizes decreased slightly when leveling up the amount of organic groups in the mesopores (Table 1).

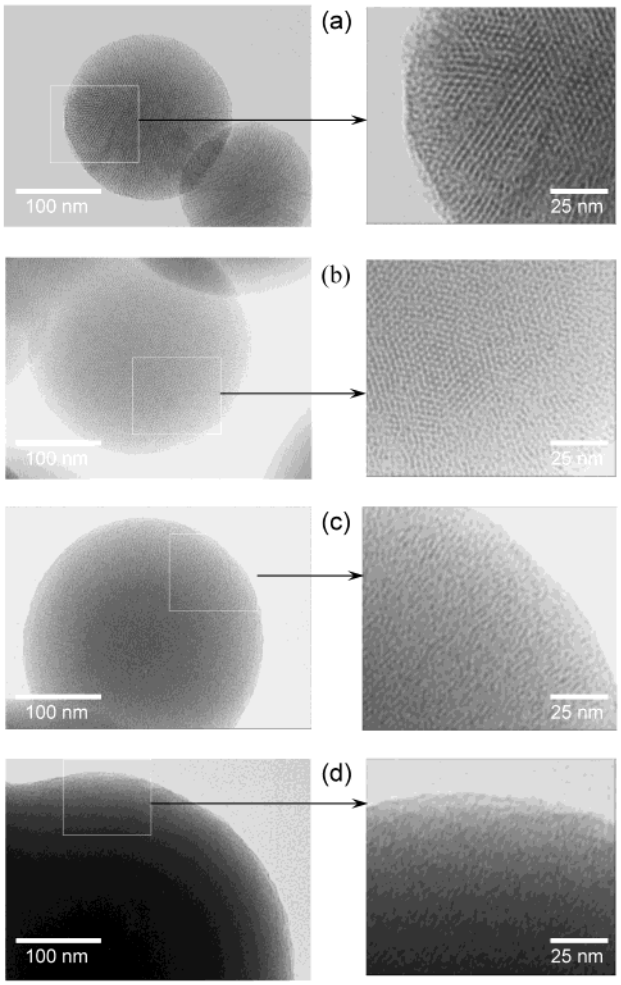

Figure 2. TEM micrographs of some surfactant-extracted nanoporous silica derivatives: (a) MCM-41, (b) MPS-5%, (c) MPS-20%, and (d) MPS-40%.

(21) Margolese, D.; Melero, J. A.; Christiansen, S. C.; Chmelka, B. F.; Stucky, G. D. *Chem. Mater.* **2000**, *12*, 2448.
(22) (a) Mori, Y.; Pinnavaia, T. J. *Chem. Mater.* **2001**, *13*, 2173. (b) Richer, R.; Mercier, L. *Chem. Mater.* **2001**, *13*, 2999. (c) Beaudet, L.; Hossain, K.-Z.; Mercier, L. *Chem. Mater.* **2003**, *15*, 327.

Increasing further the fraction of organosilane in the reaction mixture (up to 50% MPTMS) resulted in the formation of mesoporous wormhole framework structures, exhibiting a characteristic single low-angle XRD peak (Figure 1, curves d−i), similarly to what was previously observed for hybrid materials synthesized via the neutral amine route.[22a] The resulting particles were still sphere-shaped (Figure 2, part c and d) and most of the organosilane introduced in the synthesis medium (>95%) was incorporated in the final products, as pointed out by elemental analysis (Table 1). This was also confirmed by ^{29}Si NMR: distinct resonances were observed for the siloxane [Q^n = Si−(OSi)$_n$−(OH)$_{4-n}$, n = 2−4; Q^4 at −110 ppm, Q^3 at −101 ppm] and organosiloxane [T^m = RSi−(OSi)$_m$−(OH)$_{3-m}$, m = 1−3; T^3 at −65 ppm, T^2 at −56 ppm] species. Regardless of the efficiency of the organosilicon incorporation into the hybrid structures, it is noteworthy that increasing the MPTMS/TEOS stoichiometry induced restriction of the long-range structural order (increased structure defects, decreased length of the one-dimensional mesopores). Amorphous solids were formed when using 70% or 100% MPTMS in the starting sol (flat XRD patterns, see Figure 1, curves j and k), in agreement with a previous investigation reporting the absence of mesostructure formation when the synthesis mixture contained a fraction of organosilane higher than 60%.[22a]

Nitrogen adsorption−desorption isotherms for all products are provided in Figure 3, displaying also the variation of specific surface area and total pore volume with respect to the relative MPTMS/TEOS stoichiometry. All ordered materials showed type IV isotherms[23] (especially well-defined for the hexagonal MCM-41 samples), which are characteristic of mesoporous solids, the condensation step being, however, less developed for higher extent of functionalization. The hybrid samples exhibited virtually no hysteresis loops at low p/p_0 values, suggesting a rather homogeneous distribution of the organic groups in the mesopores. Nitrogen adsorption measurements of MPS materials obtained from fractions of organosilane larger than 25% yielded type I isotherms,[23] which are more typical for microporous solids. As a result of increasing amounts of organic groups in the channels, the pore volume was found to decrease continuously to reach almost zero for the MPS-70% and MPS-100% samples (Figure 3, part b). This parameter defining the free space available for reactants to reach the active sites inside the porous material is expected to affect significantly the reaction rates in such confined medium, as previously discussed for organic−inorganic hybrids based on grafted silicas.[15] The effect of functional group density on the specific surface area followed the same trend, except for the hexagonal MCM-41-type samples characterized by low loadings of mercaptopropyl moieties (Figure 3, part b). In the latter case, the presence of some organic chains, separated enough from each other, contributes to slightly increasing the internal surface area of the mesopore channels. The pore volume was essentially due to the contribution of the framework. The textural porosity, which can arise from a spongelike nature of the particles,[24] was negligible, as otherwise supported by the TEM pictures (Figure 2). The high surface areas and pore volumes measured from the isotherm data recorded for MPS samples characterized by thiol loadings in the 5−30% range, and to a lesser extent for MPS-40% and MPS-50%, agree well with the expected properties of ordered mesoporous materials.[4,11,22]

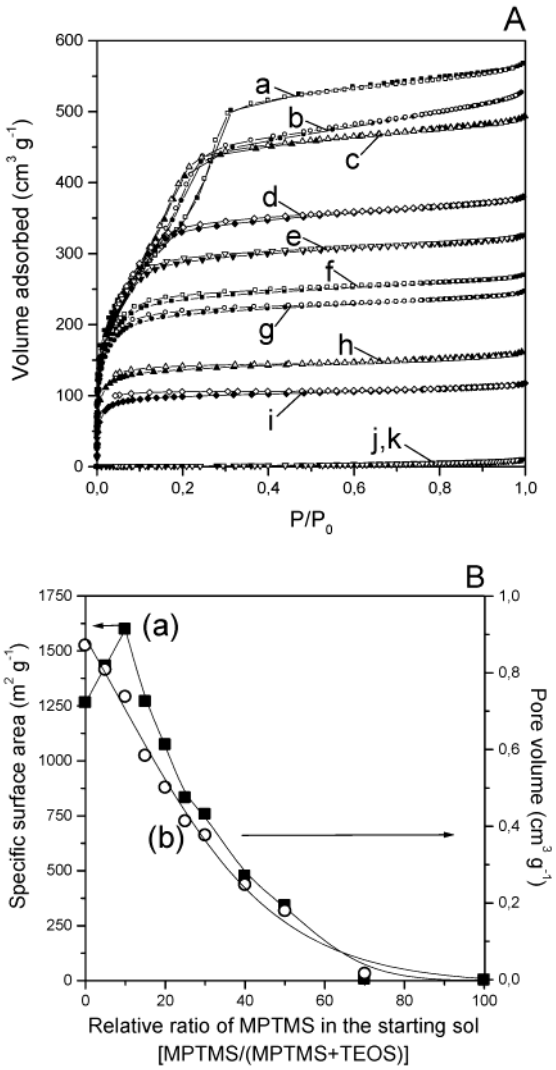

Figure 3. (A) Nitrogen adsorption isotherms obtained for the same nanoporous silica derivatives as in Figure 1. (B) Variation of (a) specific surface area and (b) total pore volume, as a function of the relative molar ratio of MPTMS in the starting sol.

Consistent with the results reported previously for the synthesis of organically modified silicas in water/ethanol mixtures containing ammonia as the catalyst,[18] the SEM images and particle size distribution measurements of the adsorbents (e.g., Figure 4) revealed that all samples possessed a spherical morphology with narrow size distribution centered around 550−600 nm. These uniform spheres, however, have a tendency to aggregate when deposited on a solid support as required to get the SEM images (Figure 4, part B). Ultrasonic treatment after dispersion in aqueous suspension led to the separation of most aggregates into isolated

(23) Greg, S. J.; Sing, K. S. W. *Adsorption, Surface Area and Porosity*, 2nd ed.; Academic Press Inc.: San Diego, CA, 1982.

(24) Zhang, W.; Pauly, T. R.; Pinnavaia, T. J. *Chem. Mater.* **1997**, *9*, 2491.

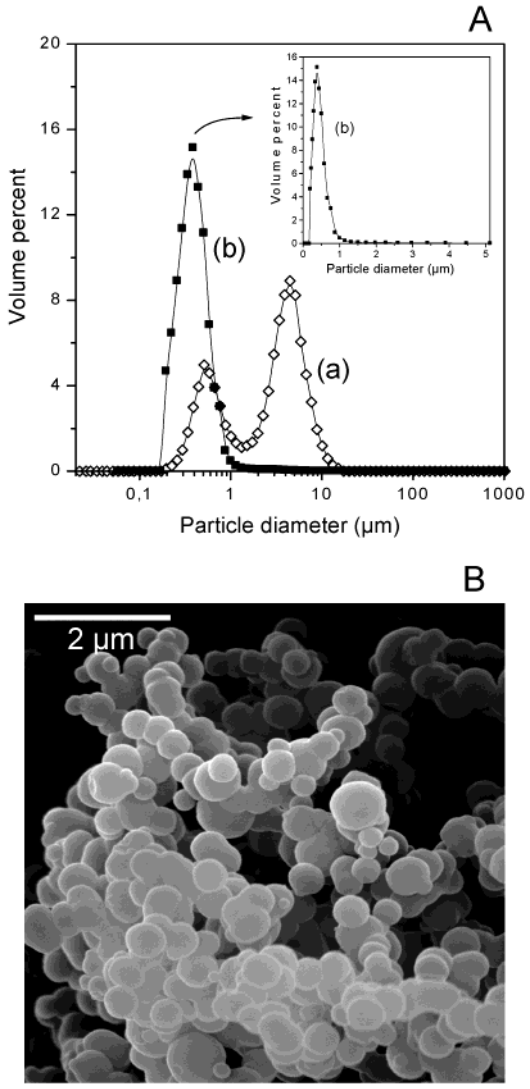

Figure 4. (A) Particle size distributions (expressed in (a) volume or (b) number) of MPS-5% sample after ultrawave treatment during 2 min. Inset: enlargement of the number distribution. (B) SEM micrograph of an aggregate of the MPS-5% sample.

individual particles and smaller aggregates. Particle size analysis revealed bimodal distribution centered around 550−600 nm for isolated spheres and 5−15 μm for closely associated particles, when expressed in volume, whereas the data presentation with respect to the number of particles confirms a narrow size distribution, centered at the mean diameters of about 550−600 nm (Figure 4, part A). Whereas the size of isolated spheres was almost constant for all samples (only a slight decrease was observed by passing from MPS-5% to MPS-100%, see Table 1), the aggregates were significantly larger for materials containing higher loadings of organic group (Table 1). This can be ascribed to increased hydrophobicity of these hybrids compared to those materials containing no or little organic moieties in their framework.

In conclusion, a series of thiol-functionalized silicates have been prepared, bearing a wide range of organic group contents and displaying either a high degree of structural organization (hexagonal MCM-41-type materials), or wormhole framework structures with long or short range order, or no order at all (amorphous solids). These organic−inorganic hybrids are also characterized by different porosity and hydrophobicity. This set of samples should therefore help to determine the main parameters that are governing the reactivity of organically modified silicates obtained by the co-condensation route in the presence of a structure-directing agent, including accessibility to the active sites and mass transfer kinetics.

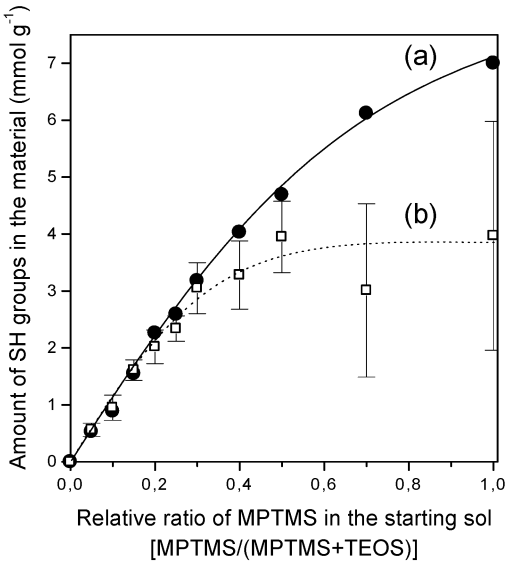

Figure 5. Variation of the amount of mercaptopropyl groups in MPS materials, as a function of the relative molar ratio of MPTMS in the starting sol, expressed as (a) total amount per mass of MPS, and (b) amount of SH groups accessible to Hg^{II}.

3.2. Accessibility to the Binding Sites − Hg^{II} Adsorption Isotherms. It is now well established that the ability for a target reactant to reach the organic active sites within porous organic−inorganic hybrids is dramatically improved when functionalization is performed on the internal surfaces of ordered mesoporous materials in comparison to the corresponding amorphous solids.[11−15] The influence of fine structure and density of functional groups on such parameter remains, however, incompletely described.

Figure 5 provides data relative to the maximum uptake of Hg^{II} by MPS materials as a function of the fraction of organosilane used for their preparation (after 24 h reaction). It also compares the experimental values to the theoretical capacity calculated on the basis of the amount of thiol ligands in the functionalized materials. As shown, the Hg^{II} loading capacity was nearly identical to the amount of thiol groups in the adsorbents up to 30% organosilane content, demonstrating the unhindered access of the metal species to all the binding sites located within the mesoporous materials. This is explained by the ordered structure of these MPS-5% to MPS-30% samples, which are characterized by better accessibility than in related porous materials with disordered networks.[11a−d,e−j,l,m,s,t] The advantage of well-defined mesopore channels seems to be independent of whether the mesostructure was hexagonal (MPS-5%, MPS-10%) or made of typical wormhole motif mesostructured phases (MPS-15% to MPS-30%).

By increasing further the funtionalization stoichiometry, the maximum Hg^{II} loading capacity leveled off at a value of about 3.8 mmol g^{-1} (Figure 5). This value

corresponds to nearly 750 mg of mercury per g of adsorbent (i.e., 43% of the total weight of Hg^{II}−loaded MPS is due to the metal species), constituting among the highest sorption capacities ever reported.[11l] For sake of comparison, the best performances reported to date have been achieved with thiol-functionalized monolayers on mesoporous silica (2.5 mmol g^{-1}),[11a] or with two kinds of thiol-functionalized silica-based materials obtained by the co-condensation route (2.3 mmol g^{-1} for MSU-2[11l] and 2.1 mmol g^{-1} for MCM-41[25]). One should also mention a recent work reporting the value of 1284 mg/g (6.4 mmol g^{-1}) by using a thiol-functionalized organoceramic amorphous adsorbent prepared from the co-condensation of MPTMS and TEOS in 1:2 ratio,[25] which appears, however, unrealistic on the basis of the maximum thiol content of a material obtained from such a precursor ratio. In contrast to the well-ordered mesostructures, less-than-complete complexation was thus observed for less ordered adsorbents (MPS-40% to MPS-100%). This can be explained by the increasingly irregular pore channels arising from the presence of increasing amounts of organic groups in the material, which is likely to induce pore blocking as in grafted amorphous silica gels,[11b,15a] but also by the possible existence (in the highly functionalized MPS samples) of a fraction of mercaptopropyl groups located inside the silica walls (and not on the pore surface) which remain, therefore, inaccessible to bind Hg^{II} species. Another suspected limitation is the formation of noncomplexant dipropyl-disulfide moieties that may arise from the oxidative coupling of two adjacent thiol groups[26] (even if they were not evidenced by Raman spectroscopy, they are expected to occur more probably as the higher is the density of mercaptopropyl groups in the material). It is also noteworthy that a great dispersion of adsorption data was observed for MPS-70% and MPS-100% samples because of the difficulty of homogeneously suspending the highly hydrophobic particles in an aqueous medium.

Figure 6 depicts the adsorption isotherms showing the molar quantity of Hg^{II} species immobilized by 20 mg of several MPS adsorbents as a function of the initial amount (total Hg^{II}) in solution. It covers a wide range of Hg^{II} concentrations, working either in excess Hg^{II} with respect to the MPS capacity or using lower Hg^{II} amounts. The dashed line represents the unity slope denoting the quantitative adsorption. As shown, very efficient binding of Hg^{II} by all the MPS materials was observed, reducing the residual metal concentration in solution to very low values (<0.1 μM) when the amount of solution-phase Hg^{II} was below the saturation level of MPS. As expected from results of Figure 5, the efficiency of the uptake process continuously increased in proportion to the SH content in MPS. As previously observed for other functionalized mesoporous ion adsorbents,[11b] progressive reduction of pore volume of MPS materials was observed upon filling with Hg^{II} species. It is noteworthy that MPS materials suffered somewhat from lack of quantativity when approaching their total loading capacity (some splitting between the experimental adsorption curves and the theoretical

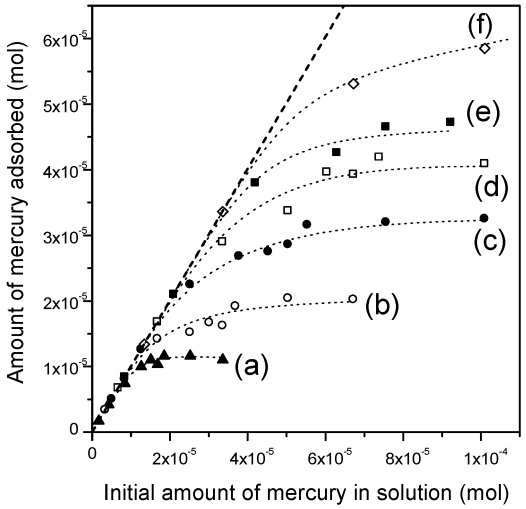

Figure 6. Adsorption isotherms for Hg^{II} on various MPS samples: (a) MPS-5%, (b) MPS-10%, (c) MPS-15%, (d) MPS-20%, (e) MPS-25%, and (f) MPS-40%, expressed in terms of the amount of adsorbed species as a function of the total amount of Hg^{II} in the starting solution. Experimental conditions: 20 mg MPS in 0.1 M HNO_3 solution (20 mL).

quantitative slope can be noticed at filling extents higher than 70−80%, see Figure 6, and this is especially marked for high-capacity adsorbents). When expressed with respect to the equilibrium Hg^{II} concentration in solution after 24 h reaction, all the isotherms exhibited systematically an evolution close to that typical of Langmuir behavior, in agreement with most of the previous studies on Hg^{II} adsorption using MPS mesostructures.[11b,c,j,l] This indicates a rather high binding energy of the Hg^{II} species to the active sites. Some differences between the adsorption profiles and Langmuirian behavior were observed, however, when reaching loading values close to the maximum capacity of MPS materials, suggesting some decrease in the binding energy due to difficulties of Hg^{II} to reach the binding sites located deep in a particle that was already loaded with a huge amount of metal species. This was even more evident for materials characterized by a high degree of functionalization because they induce ess easy access of the solution-phase Hg^{II} species to the active centers. Such effect of restricted reaction was reported to be especially overwhelming in highly ordered mesostructures displaying large particle sizes.[11c,t] In contrast to the results obtained with these MPS materials containing the thiol groups uniformly distributed in the mesostructures, no limitation was observed with using hybrid materials prepared by grafting mercaptopropyl groups on or within as-synthesized mesoporous silicas. This can be explained by the fact that this latter method of functionalization leads essentially to a large proportion of binding sites located at the outermost surface of particles (i.e., at the entry of mesopores, not deep in the material),[17b,26] which does not contribute to lowering the energy of the binding reaction associated with the active sites located deeper in the materials.

3.3. Factors Affecting the Speed of Hg^{II} Uptake by MPS Materials. The rate of Hg^{II} uptake by MPS materials was investigated following the same procedure as that applied to characterize the kinetics associated with the binding of Hg^{II} species to either amor-

(25) Lee, J. S.; Gomez-Salazar, S.; Tavlarides, L. L. *React. Funct. Polym.* **2001**, *49*, 159.
(26) Lim, M. H.; Blanford, C. F.; Stein, A. *Chem. Mater.* **1998**, *10*, 467.

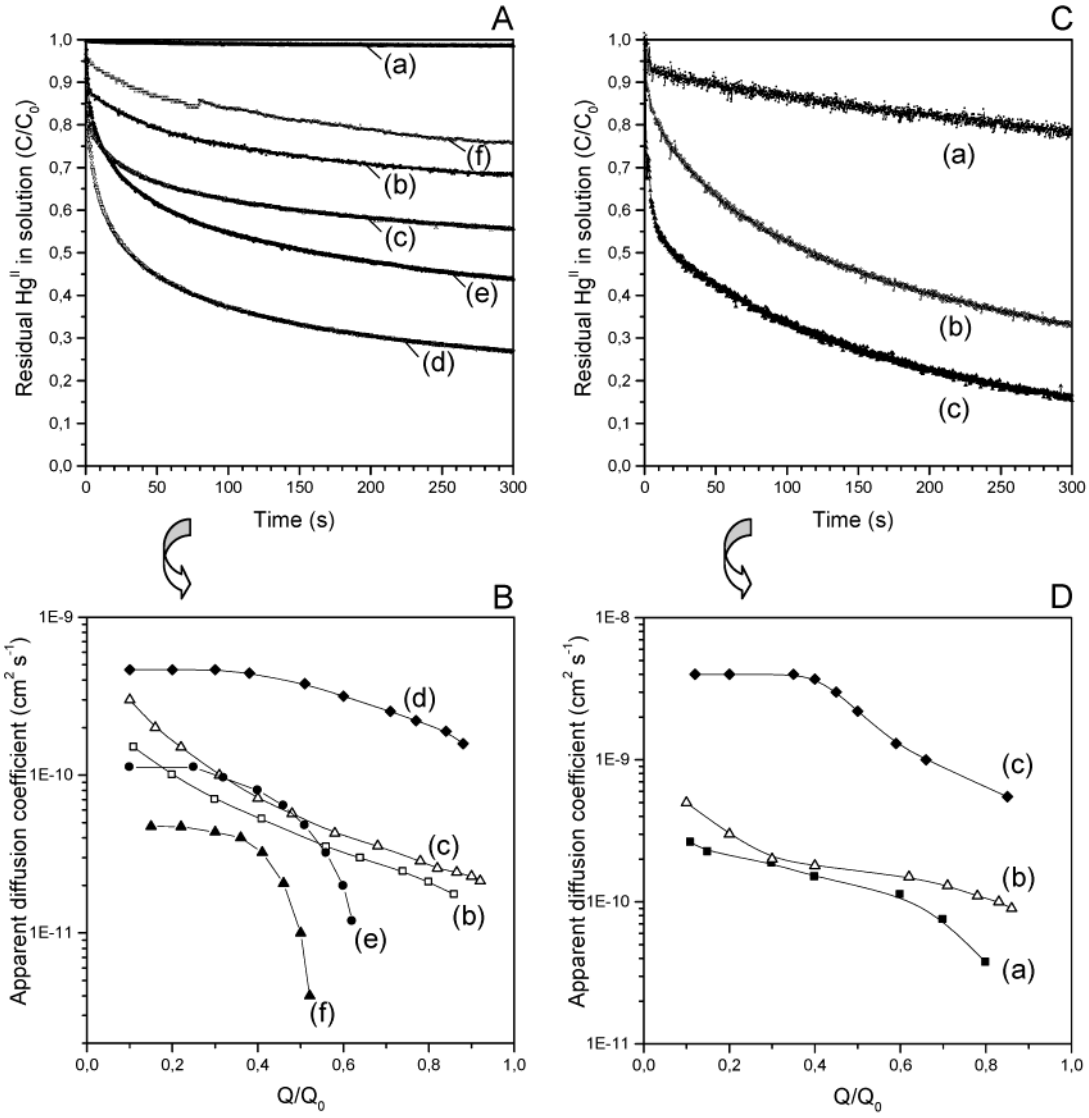

Figure 7. (A) Uptake of Hg^{II}, as a function of time, by (a) MCM-41 (0%), (b) MPS-5%, (c) MPS-10%, (d) MPS-25%, (e) MPS-40%, and (f) MPS-70%, from solutions containing Hg^{II} at an initial concentration selected to correspond to the maximal amount of accessible −SH groups in each material (as measured after 24 h reaction, see Figure 5). (B) Corresponding variation of the apparent diffusion coefficients as a function of the extent of reaction; $Q_0 = 1$ is defined with respect to the experimentally observed maximal capacity for each material for Hg^{II} species (as in Figure 5), while Q corresponds to the fraction of complexed ligand. (C) Same as A for samples (a) Geduran-SH, (b) MCM-41-SH, and (c) SBA-15-SH. (D) Same as B for (a) Geduran-SH, (b) MCM-41-SH, and (c) SBA-15-SH.

phous silica gels or ordered mesoporous MCM-41 samples grafted with mercaptopropyl groups, i.e., by in situ monitoring of Hg^{II} consumption from aqueous suspensions of MPS as a function of time by fast electrochemical measurements.[15] Typical results for some MPS samples are shown in Figure 7 (part A), including comparative data obtained with grafted materials (part C). They are presented in the form of a C/C_0 vs t plot where C is the remaining solution-phase Hg^{II} concentration at time t and C_0 is its initial concentration before adding the MPS particles in the medium. All these data have been obtained by adjusting the solid/solution ratio in such a way that the initial amount of Hg^{II} in solution corresponds exactly to the maximal amount of Hg^{II} that can be adsorbed by each MPS sample (it means that all these curves tended to $C = 0$ at $t = 24$ h, except for the unmodified MCM-41 which never adsorbed more than 5% of solution-phase Hg^{II} under the experimental conditions used in this study). Similar experiments have been repeated for each MPS sample by adjusting the Hg^{II} concentration in solution to 50% of the loading capacity of the adsorbents, to get more accurate data in the early times of the uptake process.

Figure 7A shows that the speed at which Hg^{II} species are adsorbed by MPS materials is very dependent on the adsorbent type (structure and density of functional groups). It seems at first glance that fastest mass transfer rates were observed with the MPS-25% sample, while lower uptake efficiencies were achieved for MPS solids of either lower or higher loading capacity. Slower diffusion kinetics associated with the materials displaying high density of thiol groups and poor structure are consistent with our previous studies on grafted silicas for which ordered mesoporous solids gave rise to access rates to the binding sites faster than in the amorphous ones (see, e.g., Figure 7C) as well as enhanced diffusion rates by decreasing the amount of grafted ligands or increasing pore size.[15] Such resistance to mass transport

is clearly due to stronger steric constraints and to higher hydrophobicity due to the high organic group contents. However, the fact that the reaction rates are apparently slower when using MPS displaying a lower density of thiol groups, a greater porosity, and a more ordered structure, is somewhat intriguing (even if one could argue that low surface coverages induced a rather high population of residual silanol groups, which are expected to interact with Hg^{II} species[27] and thus to slow their movement through the MPS matrix). Anyway, the Hg^{II} uptake curves presented in Figure 7A are indicative of quite rapid processes, in contrast to the sluggish adsorption reported elsewhere for thiol-functionalized mesoporous silica spheres of relatively big size (10−12 μm).[11t] To provide a careful interpretation and discussion on mass transport processes in these mesoporous organic−inorganic hybrids, it is of course necessary to take into account their particle size.

This has been made, as previously described for grafted silicas,[15] through the calculation of the apparent diffusion coefficients, D_{app}, by fitting the kinetic curves in a first approximation according to a spherical diffusion model (eq 1).[20] This approach is valid for studying diffusion processes in the mesoporous spheres of monodisperse size considered here, at least if one considers the pore structures as fully interconnected in the different particles. As these latter have tendency to aggregate, however, calculations have been performed after measuring the particle size distribution in the same conditions as those applied in the kinetic experiments, to get reliable data, and by considering roughly the aggregates as spherical. D_{app} values are therefore related to both intra- and interparticle diffusion (there is unavoidably some void space inside the aggregates), but the rate-determining step is expected to be the speed of mass transport in the mesopores (intraparticle diffusion) because the interparticle porosity (due to the spatial arrangement of $\sim\mu$m sized particles) is greater by 2−3 orders of magnitude than that experienced by Hg^{II} species within the individual mesostructured spheres. D_{app} values have been plotted as a function of the extent of the uptake process (D_{app} values vs Q/Q_0).

The most emerging trends can be summarized from the results presented in Figure 7B, depicting the variation of D_{app} values for several MPS materials as a function of their occupancy level. The first feature, common to all samples, is a continuous decrease in diffusivity upon filling with the heavy metal; this can be explained by increasing steric constraints in the MPS material as far as metal adsorption proceeds, in agreement with the concomitant decrease in its total pore volume. Such hindered ingress was also observed in grafted silica-based materials (e.g., Figure 7, part D).[15] In this case, however, the shape of the D_{app} vs Q/Q_0 plots was found to be strongly dependent on the materials type.

A continuous decrease of D_{app} was observed as far as the uptake process was going on with well-organized MCM-41-type MPS materials containing rather low levels of thiol groups (MPS-5% and MPS-10%, see curves b & c on Figure 7B). These adsorbents were really mesoporous (pore size ≥ 2 nm, see Table 1) and the progressive filling of their uniform mesopores did not lead to any pore blocking phenomenon; the continuous decrease of D_{app} being explained by the progressive decrease of free space available in the mesostructure for diffusion of the analytes by increasing the mercury occupancy level. Such variation is quite similar to that observed for small-pore MCM-41 (≈3 nm) grafted with the same mercaptopropyl ligands (curve b on Figure 7D), with, however, a larger slope most likely due to the presence of thiol groups uniformly distributed over the whole pore volume of the material (inducing higher mass transfer resistance to more ligands located in the bulk MPS material in comparison to easier access to a large number of ligands located at the entry of mesopores in grafted materials). No synergistic acceleration of the uptake rate was pointed out with increasing the metal ion loading of the small MPS microspheres, contrary to what was reported for diffusion kinetics in larger mesoporous organosilica spheres.[11t] D_{app} values calculated here for Hg^{II} diffusion in small MPS-5% and MPS-10% spheres are larger by 1 order of magnitude than those reported for the larger thiol-functionalized mesoporous spheres (MSU-type, 2−6% MPTMS)[11t] prepared under mildly acidic nonionic surfactant solutions in the presence of fluoride catalyst.

When increasing the density of functional groups in the hybrid materials, significant changes in the D_{app} vs Q/Q_0 profiles were observed, as illustrated in Figure 7B for MPS-25%, MPS-40%, and MPS-70%. D_{app} values calculated at the early times of the uptake process were quite independent of Q/Q_0, whereas those measured at higher occupancy levels dropped dramatically. They dropped more abruptly and rapidly (i.e., at lower Q/Q_0) as the MPS materials contained a high content of organic groups. Moreover, D_{app} was always lower in materials of higher degree of functionalization. All these observations are consistent with hampered transport of solute in confined media: (1) increasing the density of functional groups induced lowering of total pore volume and pore size (Table 1) and higher hydrophobicity of the material (confirmed by slow adsorption of water on MPS[11r]), limiting therefore the rate of access to the binding sites; (2) complexation of thiol groups by Hg^{II} species resulted in a decrease of the remaining free space in the mesopores, which may even lead to pore blockage at a certain occupancy level, explaining the sharp slackening of the uptake rates; (3) this dropping of D_{app} values occurred at filling levels all the more low as the pore volume of the MPS material was smaller. Pore volumes measured at Q/Q_0 levels above the breakthrough of D_{app} values were always lower than 0.05 $cm^3\ g^{-1}$. So strong diffusional limitations were also reported for organically modified MCM-41 samples in which hierarchical polymerization of the organosilane had been allowed. One should finally mention that the advantage of a uniformly ordered mesoporous structure in vastly improving reaction rates in comparison to the corresponding amorphous solids[15] is valid only for open mesostructures containing a density of ligand at a maximum threshold level above which the kinetics associated with the transport of solutes to the binding sites becomes dramatically restricted as a consequence of mesopore occlusion.

(27) Walcarius, A.; Devoy, J.; Bessière, J. *Environ. Sci. Technol.* **1999**, *33*, 3, 4278.

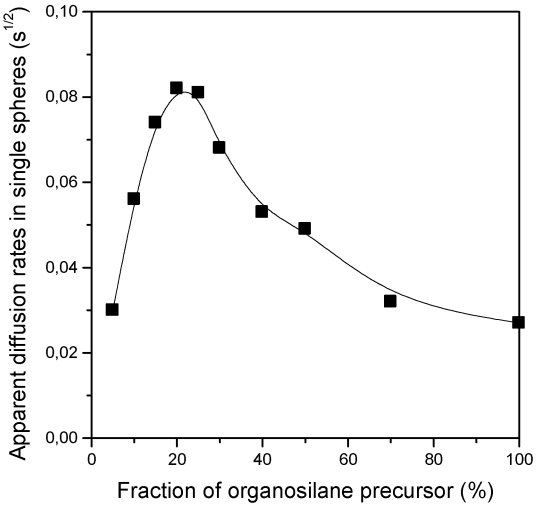

Figure 8. Variation of the apparent diffusion rates of Hg^{II} in isolated MPS spheres as a function of the relative molar ratio of MPTMS in the starting sol; data were estimated from kinetic curves at the early times of the experiments when the uptake process is dominated by the smaller particles (slope of the Q/Q_0 versus $\sqrt{t}$ plot, calculated at $Q/Q_0 \rightarrow 0$).

All the above results and discussions are based on D_{app} values calculated from a diffusion model taking into account the particle size distribution of both MPS particles and aggregates in suspension (i.e., the real case covering the whole Q/Q_0 range). However, as a significant part of the adsorbents (15−30% depending on the functionalization degree) does exist in the form of individual spheres of monodisperse size in suspension, these small particles in comparison to the bigger aggregates are expected to control the uptake process at the early stage of the experiments (the particles located on the outermost surface of the aggregates also belong to this part of easily accessible sites). In other words, reaching the binding sites located in a mesoporous spherical particle situated in the bulk of an aggregate would be achieved well after the complete filling of an individual small sphere suspended freely in the solution. One can therefore use the data gathered at the beginning of the uptake experiments to characterize the mass transfer rates in individual MPS microspheres. The relative speed of Hg^{II} binding to MPS microspheres as a function of their functionalization degree is depicted in Figure 8 (slope of the Q/Q_0 vs $\sqrt{t}$ plot, which is linear at the early stage of diffusion in a sphere[20]). This picture features clearly three domains of variable rates of access to the binding sites in organically modified silicates obtained by the co-condensation route: (1) despite the fact that ordered mesoporous silicas grafted with organic groups displayed definitely higher rates of access to the binding sites than in corresponding amorphous solids,[15] some restrictions have been observed with highly ordered mesoporous hybrids obtained by one-pot synthesis, at least when they displayed long-range structuration inducing the presence of binding sites located deep in long mesopore channels (MPS-5%, MPS-10%); (2) in contrast, mass transport rates in functionalized mesoporous solids displaying wormhole framework structures with shorter-range order were found to be dramatically faster (MPS-15% to MPS-30%), arguing further to support the relationships existing between reactivity and long-range structural order/disorder, which was first discussed by Pinnavaia et al.[14d] for mesoporous molecular sieve catalysts (although the exact evaluation of the mesopore length may be difficult, improved communication through the wormhole-like mesostructures made of interconnected three-dimensional pore networks is expected to occur, in comparison to that in hexagonally packed one-dimensional channels of MCM-41, as otherwise sustained by more effective diffusion processes in ordered mesoporous materials with interconnected mesotunnels[28]); (3) finally, the MPS materials containing very high organosilane contents (>30%) are characterized by rather weak cristallinity, low porosity, and high hydrophobicity, inducing significant resistance to mass transfer through their porous network with a concomitant dramatic decrease in diffusion rates.

4. Conclusions

Mass transport issues in porous organically modified silica spheres obtained by the co-condensation route are strongly influenced by the framework structure of the materials and the density of functional groups. This has been demonstrated here for the uptake of Hg^{II} species from aqueous solutions by a wide range of mercaptopropyl-functionalized silica adsorbents prepared by the sol−gel method in the presence of a surfactant templating agent, by varying the MPTMS/TEOS ratio in the synthesis medium.

Basically, one can distinguish three categories of adsorbents. (1) Those characterized by a well-ordered MCM-41 structure over a rather long range, which can be obtained only with low MPTMS contents (up to 10%), which resulted in a complete accessibility to all their binding sites; but they underwent some restrictions to mass transport, especially for reaching the active centers located deep in the one-dimensional mesopore channels; (2) Those displaying less-ordered structures, but still made of cylindrical mesopores organized in a wormhole-like three-dimensional arrangement, which were characterized by significantly faster diffusion rates despite their lower pore volumes. The quantitative access to all the binding sites was observed up to MPS-30%, while higher functionalization degrees gave rise to less-than-complete filling because of steric hindrance and/or high hydrophobicity. Nevertheless, these adsorbents with high density of functional groups led to very high sorption capacities for Hg^{II} species (up to 750 mg g^{-1}). (3) Those materials containing the highest thiol group contents were poorly ordered or even totally amorphous and they were subject to dramatic restriction of mass transport rates as well as limited accessibility to the binding sites.

In agreement with the decrease in pore volume concomitant to the uptake process and the rather long times to get full filling of the organosilicas, the apparent diffusion coefficients for Hg^{II} in all the MPS samples were found to decrease as far as the reaction was going on, and faster as the degree of functionalization was higher.

(28) (a) Fan, J.; Yu, C.; Wang, L.; Tu, B.; Zhao, D.; Sakamoto, Y.; Terasaki, O. *J. Am. Chem. Soc.* **2001**, *123*, 12113. (b) Lin, H.-P.; Wong, S.-T.; Liu, S.-B.; Mou, C.-Y.; Tang, C.-Y. *Stud. Surf. Sci. Catal.* **2000**, *129*, 15.

Long-range versus short-range structural order/disorder in organically modified mesoporous silica spheres, which can be induced by varying their degree of functionalization, is thus a key parameter affecting the speed of access of reactants to the active centers. Focusing on the MPS−Hg^{II} system, this work provides an illustration of how to obtain hybrid materials displaying either the highest sorption capacity or the fastest access to the binding sites. It is anticipated that such an approach may contribute at increasing the performance of mesoporous organic−inorganic hybrids in various fields including separation sciences, sensors, or heterogeneous catalysis.

Acknowledgment. We gratefully acknowledge J.-P. Emeraux for recording XRD spectra, A. Koller for SEM images, and J. Ghanbaja for TEM experiments, as well as B. Lebeau and M. Etienne for fruitful discussions on the field of mesoporous organic−inorganic hybrids.

CM031089L